BMB Reports - Manuscript Submission

Manuscript Draft

Manuscript Number: BMB-16-185

Title: Survivin protects fused cancer cells from massive cell death

Article Type: Article

Keywords: Cell fusion; Cell death; Apoptosis; Proliferation; Survivin

Corresponding Author: Jae-Ho Lee

Authors: Mihyang Do[1,2,3], In-Hae Kwak[1], Ju-Hyun Ahn[1,2,3], In Jeong Lee[1], Jae-Ho Lee[1,2,3,*]

Institution: [1]Department of Biochemistry and Molecular Biology, Ajou University School of Medicine,
[2]Department of Biomedical Sciences, The Graduate School, Ajou University,
[3]Genomic instability Research Center, Ajou University School of Medicine,

Manuscript Type: Article

Title: Survivin protects fused cancer cells from massive cell death

Author's name: Mihyang Do[1,2,3], In-Hae Kwak[1], Ju-Hyun Ahn[1,2,3], In Jeong Lee[1] and Jae-Ho Lee[1,2,3*]

Affiliation: [1]Department of Biochemistry and Molecular Biology, [2]Genomic instability Research Center, Ajou University School of Medicine, [3]Department of Biomedical Sciences, The Graduate School, Ajou University, Suwon 16499, Korea.

Running Title: The role of survivin in cell death of fused cells

Keywords: Cell fusion; Cell death; Apoptosis; Proliferation; Survivin

Corresponding Author's Information:

Tel: +82 31 2195053; Fax: +82 31 2195059; E-mail: jhlee64@ajou.ac.kr

ABSTRACT

Tetraploidy, a potential precursor of cancer-associated aneuploidy, is produced either by cell fusion or cytokinesis failure. Here, we used low p53-expressing HeLa cells to address the fate of cancer cells after fusion. We found that massive cell death or growth arrest occurred a few days after fusion. Interestingly, cells with larger nuclei preferentially died after fusion, suggesting that a larger deviation of DNA content is a strong inducer of apoptosis. Notably, a fraction of cells escaped cell death. It turned out that the stability of survivin was increased, and its localization changed preferentially to the cytosol in fused cells. Knockdown of survivin decreased survival more in fused cells than in unfused ones, showing more dependency of fused cells on survivin. Collectively, after cancer cell fusion, some fused cells can avoid apoptotic crisis partly owing to survivin and proliferate continuously, a process that might contribute to human cancer progression.

INTRODUCTION

Physiological cell fusion results in terminally differentiated cells, such as syncytiotrophoblasts, myocytes and osteoclasts, whereas unphysiological cell fusion induced by a variety of agents, including viruses and chemicals, produce fused cells with proliferative capacity (1). As a result of subsequent cell divisions, these fused tetraploid cells give rise to daughter cells that exhibit genomic instability, a process similar to the genomic instability that follows cytokinesis failure, which causes daughter cells to become aneuploid and carcinogenic (2).

Unphysiological cell fusion has also been considered a mechanism by which cancer cells acquire more aggressive phenotypes (3). For example, fusion of cancer cells with

macrophages has been reported to confer on cancer cells the capacity to invade and metastasize (4). It has also been suggested that fusion of cancer cells with endothelial cells may enable cancer cells to more easily penetrate the endothelial cell layer (5). Importantly, fusion between cancer cells can induce genomic instability, which can be a driving force for these cells to obtain diverse tumor-progression phenotypes (3).

The tetraploid cells produced by either cell fusion or cytokinesis failure become cell cycle-arrested or apoptotic through a process that has been considered to be p53 dependent (6-8). Activation of p53 induces p21-dependent cell-cycle arrest or increases proapoptotic Bcl-2 family proteins, such as Bax and Puma/BBC3, and thus induces apoptosis in a cell context-dependent manner (9-11). Therefore, after cell fusion or cytokinesis failure, those cells with increased p53 activity are removed (8), whereas cells in which p53 is less activated survive and even proliferate, demonstrating an ability to form colonies in soft agar (12). Considering the tendency of cancer cells to inactivate p53, fusion between cancer cells may result in a high probability of escaping cell cycle arrest and/or cell death after fusion, while simultaneously allowing acquisition of proliferative potential and genomic instability. Therefore, understanding the fate of cells arising from the fusion of cancer cells with decreased p53 activity is important to understanding the role of cancer cell fusion in cancer progression. In addition, the factors that determine the fate of fused cells are also important, but have not yet been identified.

Here, we used HeLa cells, which harbor low levels of p53 owing to enhanced p53 degradation in the presence of the E6 viral oncoprotein, as a model system to address the fate of cancer cells after fusion in the context of decreased influence of p53 (13). Interestingly, massive cell death occurred a few days after fusion, followed by the

emergence of proliferating cells. These proliferating cells were mainly originated from the fusion of two cells and appeared to have escaped apoptotic cell death, which had eliminated cells with a higher DNA content. Furthermore, upregulation and cytosolic localization of survivin was at least partly responsible for the escape of these proliferating cells from apoptotic crisis.

RESULTS

Fused cells experience massive cell death and growth arrest.

Separate populations of Geneticin-resistant and hygromycin-resistant HeLa cells were stained with the vital fluorescence dye DiO and DiI, respectively, and then subjected to electrofusion. Fused cells and unfused cells were separated and isolated by fluorescence-activated cell sorting (FACS). Dio(+)/DiI(+) cells were identified as fused cells, whereas DiO(-)/DiI(+) cells corresponded to unfused cells, which were used as control cells that had undergone the electrofusion procedure but without the resultant cell fusion (Supplementary Fig. 1A). Fused and unfused cells were easily differentiated under a fluorescence microscope (Fig. 1A), and FACS analysis revealed that ~99% of the FACS-sorted fused cells were DiO (+) and DiI (+) (Supplementary Fig. 1C), indicating the reliability of the FACS procedure. A further analysis of fused cells immediately after cell fusion revealed that 69.8 ± 2.7% had two nuclei, whereas the remaining ~30% had more than three nuclei, suggesting fusion of more than three cells (Supplementary Fig. 1B).

To address the fate of fused cells, we monitored cell proliferation and death after fusion. As shown in Fig. 1B, the growth rate of fused cells was significantly lower than that of unfused cells 4 days after cell fusion. Thereafter, the proliferation of fused cells modestly

increased, whereas that of unfused cells increased steeply. Trypan blue staining revealed that fused cells underwent massive cell death, peaking at 33.7 ± 4.0% cell death on day 4 after fusion (Fig. 1C). The subsequent decrease in the cell death rate at day 6 coincided with a gradual increase in the proliferation of fused cells. These observations suggest that the observed differences in cell proliferation might be at least partly attributable to differences in cell death.

We next followed the fate of individual cells by counting cell numbers over time in each well of a 96-well plate after limiting dilution. Whereas most unfused cells showed a steep increase in cell number per well during this period (Fig. 1D, left panel), a majority of fused cells showed a steep decline in cell number per well after variable times of division (Fig. 1D, right panel). An analysis of clones 9 days after fusion classified 81.4% of unfused cells as proliferative, 6.8% as growth arrested and placed 11.9% in the cell death category. The classification of clones of fused cells revealed a quite different picture: 26.8% were proliferative, 32.1% were in growth arrest and 41.1% belonged to the cell death category (Fig. 1E). These data clearly demonstrate that despite using cancer cells with decreased p53 activity, a major population of fused cells underwent cell death or growth arrest, whereas a fraction escaped the apoptotic crisis and continued to proliferate.

Elimination of cells with multinucleated nuclei through apoptosis.

To more precisely describe cell fates after cell fusion, we continuously monitored cells by time-lapse microscopy. This analysis clearly revealed a major population of dead (Fig. 2A, row 3) or growth-arrested cells, and a minor population of continuously proliferating cells (Fig. 2A, row 2). In contrast, most unfused cells were proliferative (Fig. 2A, row 1).

We then addressed whether DNA content affected the fate of fused cells. Since it is very difficult to directly measure DNA content from time-lapse data using GFP-H2B- and DsRed-H1-HeLa cells, we instead measured nuclear size as a surrogate marker for DNA content. As expected, the extent of the increase in nuclear size 1 day after fusion varied considerably. Interestingly, the heterogeneity of nuclear size observed 1 day after fusion decreased gradually together with a decrease in average nuclear size (Fig. 2B), suggesting the disappearance of cells with larger nuclei. Indeed, tracking the fate of daughter cells having same parent cells by time-lapse analysis enabled us to clearly determine that dead cells had larger nuclei compared with live cells (Fig. 2D).

It has previously been reported that tetraploid cells induced by cell fusion or cytokinesis failure tend to die by apoptosis (14, 15). To address this aspect, we assessed apoptosis by measuring levels of the active (cleaved) form of the apoptosis-inducing factors, poly (ADP-ribose) polymerase 1 (PARP-1) and caspase-3, in fused and unfused cells. As shown in Figure 2C, cleavage of PARP-1 and caspase-3 was robustly increased in fused cells, but not in unfused cells, suggesting that the death of fused cells was at least partly attributable to apoptosis. Moreover, z-VAD-fmk, a pan-caspase inhibitor, clearly abolished the cleavage of both PARP-1 and caspase-3 (Fig. 2C), and partly prevented the death of fused cells, but not unfused cells (Fig. 2E), suggesting the involvement of caspase-dependent apoptosis in the death of fused cells at least partially. Interestingly, both immunoblot and immunocytochemical assessment of p53 showed an increase in p53 levels in fused cells compared to unfused cells (Supplementary Fig. 3), indicating that even in HeLa cells, p53 levels increased after fusion and probably contributed to the massive cell death after cell fusion, suggesting that the decrease in p53 in HeLa cells

caused by HPV E6 protein can be overcome by strong apoptotic stimuli, one of which is cell fusion.

To confirm this, we checked the effect of p53 depletion on growth and death of fused cells. After p53 depletion (Supplementary Fig. 3C), cell growth was significantly increased in fused cells after day 5 post-fusion while unfused cells showed no changes by p53 depletion (Supplementary Fig. 3D). In addition, the death of fused cells after p53 depletion has showed the tendency to drop at day 3 post-fusion, and significantly dropped at day 5. On the contrary, unfused cells did not show significant decrease in cell death by p53 depletion (Supplementary Fig. 3E). Collectively, our data indicate that a majority of fused cells succumbed to death, probably owing to an increase in p53, whereas only a few cells that overcame this apoptotic crisis ultimately attained the capacity to grow continuously.

Survivin is necessary for the survival of fused cells that escape apoptotic crisis.

Since a major fraction of fused cells died through caspase-dependent apoptosis, averting apoptosis might be very important for those cells that managed to escape this crisis after cell fusion. We therefore measured the expression of various anti- and pro-apoptotic proteins after cell fusion (data not shown). As shown in Fig. 3A, the expression level of survivin, a well-known anti-apoptotic protein, was clearly increased in fused cells compared to unfused cells as early as 3 days after fusion and remained elevated throughout the experimental period. Interestingly, Bcl2 expression increased on day 7 after fusion in both unfused and fused cells for reasons that are not yet clear. To address whether the increased expression of survivin is a characteristic of surviving fused cells,

we measured survivin expression levels in stable clones of fused cells previously established by the limiting-dilution procedure. As shown in Figure 3B, all four established cell lines of fused cells showed a variable, but clear, increase in the expression of survivin, but not Bcl2 or BAG1, compared with stable clones of unfused cells, strongly suggesting that overexpression of survivin is a common characteristic of surviving fused cells.

Moreover, in colony-forming assay, two different small inhibitory RNA (siRNA) that effectively decreased survivin expression reduced the survival fraction of fused cells by 70~80% compared to control siRNA treatment, whereas knockdown of survivin in unfused HeLa cells resulted in approximately a 40~50% decrease in the survival fraction after fusion compared with control siRNA treatment (Fig. 3D). Therefore, although siSurvivin reduced cell survival in unfused cells, it exerted more effects on the survival of fused cells. Further analysis using time-lapse monitoring confirmed that knockdown of survivin reduced cell survival significantly more in fused cells compared to unfused cells (Fig. 3C). These data suggest that those fused cells that happened to overexpress survivin have the potential to avert the apoptotic crisis of fused cells, and survive to become more stable cells that can proliferate continuously.

Survivin protein in fused cells is localized in the cytosol and shows increased stability.

Next, we checked how survivin increased in fused cells. The quantitative RT-PCR analysis clearly showed no significant increase in survivin mRNA in cells following fusion (Supplementary Fig. 2B), suggesting a post-transcriptional mechanism. Therefore,

we compared survivin degradation rates in fused and unfused cells. In unfused cells, the half-life ($t_{1/2}$) of survivin protein was less than 30 minutes (26.3 ± 3.9 min), in agreement with published reports (16). However, in the case of fused cells, $t_{1/2}$ was increased significantly (48.4 ± 3.0 min, Fig. 4C).

Since cytoplasmic and/or mitochondrial survivin is considered to be cytoprotective (17), we assessed the subcellular localization of survivin by western blotting and immunocytochemical analysis. Interestingly, we observed an increase of survivin in the cytoplasmic fraction of fused cells in western blotting, resulting in approximately a 3-fold increase in the survivin cytosolic-to-nuclear ratio (Fig. 4A). Immunocytochemical analysis further confirmed the increase of cytosolic survivin in fused cells (Fig. 4B). These data clearly suggest that both the increase in protein stability of survivin and preferential localization to the cytosol contribute to the survival of some fraction of fused cells.

DISCUSSION

Tetraploidy is accepted as a potential precursor of cancer-associated aneuploidy, and considered to be a possible cause of tumor formation as well as tumor progression. Tetraploid cells can be produced either by cell fusion or cytokinesis failure. As a first step to understand the implication of cancer cell fusion in tumor progression, we tried to describe the fate of fused cancer cells and underlying molecular explanations related with cell fate. Actually, researchers already showed that most tetraploid cells resulting from non-cancerous cell fusion would undergo p53-dependent cell cycle arrest or apoptosis (6). We used HeLa cells as a model system because HeLa cells are well-known to have HPV

E6 protein (13), thus have low amount/activity of p53, which condition we frequently encounter in cancer. Interestingly, we found that massive apoptotic cell death or growth arrest occurred a few days after fusion even in HeLa cells (Fig.1 and 2), and surprisingly, it was accompanied by an increase in p53 (Supplementary Fig. 3). Induction of p53 and p53-induced cell death processes in HeLa cells has been reported previously (18, 19), suggesting that strong apoptotic stimuli could overcome E6-induced downregulation of p53. In addition, we also observed that fused cells with larger nuclei, indicating larger DNA contents, preferentially died after fusion (Fig. 2D), suggesting that a larger deviation from normal DNA content is a strong inducer of apoptosis.

Notably, a fraction of cells escaped cell death and proliferated, and these surviving fused cells were characterized by upregulation of survivin (Fig. 1, 2 and 3). Survivin is the smallest member of the inhibitor of apoptosis (IAP) family proteins, and plays a key role in inhibiting apoptosis by blocking caspase activation (20). Additionally, survivin has been reported to not only exert anti-apoptotic functions, but also cell proliferative functions, reflecting its involvement in forming the chromosome passenger complex, which is crucial for the normal progression of the cell cycle (21). Therefore, the overexpression of survivin probably affected the survival/proliferation of fused cells shortly after fusion, possibly providing fused cells the power to overcome the apoptotic crisis.

Regarding the mechanism underlying the increase in survivin, both transcriptional and post-translational regulation were majorly considered (20). It has been reported that the transcription factors SP1, E2F, and HIF-1α (hypoxia-inducible factor 1α) increase survivin expression, whereas p53 and the forkhead box transcription factors, FOXO1 and

FOXO3, decrease it (20). Notably, hypoxia upregulates both HIF-1α and survivin expression in HeLa cells (22). However, our quantitative RT-PCR analysis clearly showed no significant increase in survivin mRNA in cells following fusion (Supplmentary Fig. 2B). In relation to post-translational regulation, it has been reported that heatshock protein 90 increases the stability of survivin (23). Although we observed the delay in survivin degradation (Fig. 4), we could not observe the changes in the amount of heatshock protein 90 in fused cells (data not shown). Thus, the molecular mechanism responsible for the upregulation of survivin found here remains to be determined.

Cytoplasmic and/or mitochondrial survivin is considered to be cytoprotective (17). Interestingly, we observed an increase of survivin in the cytoplasmic fraction of fused cells (Fig. 4A and B), suggesting that both the increase in protein stability and preferential localization to the cytosol worked in fused cells. Inhibition of nuclear export of survivin by using leptomycin B, however, did not decrease the survival of fused cells in our hand (data not shown), which might be due to the non-specific effects of leptomycin B to the nuclear export of diverse array of proteins other than survivin.

In conclusion, fusion of HeLa cells induces massive apoptosis, despite the fact that the parental cells have low levels of p53. Given that survivin is overexpressed in various cancers, including breast, lung, prostate, gastric and colon cancers, and high levels of survivin expression are correlated with poor prognosis in many cancer patients (24), the survival of survivin-upregulated cells after cancer cell fusion might contribute to the progression of these types of cancers.

MATERIALS AND METHODS

See supplementary information for this data.

ACKNOWLEDGMENTS

This work was supported by the National Research Foundation of Korea (No. 2010-0011504, 2009-0076802).

CONFLICTS OF INTEREST

No conflicts.

FIGURE LEGENDS

Figure 1. Analysis of cell fate after cancer cell fusion. (A) Representative images of fused and unfused cells obtained from fusion of DiI^+- and DiO^+-HeLa cells. HeLa cells were fused as described in Materials and Methods. Bar, 50μm. (B) and (C) After cell fusion, cell proliferation and death rate were measured after trypan blue staining. Cells were seeded at a density of $1x10^4$cells per well in 12-well plates and counted at the indicated times. Mean ± SD from three independent experiments; ***, $p<0.001$; *, $p<0.05$ by Student's *t*-test. (D) The fate of individual cell was monitored under microscope. (E) At 9 day after cell seeding, cell clones were classified as either growth (wells having more than two cells/well), arrest (1~2 cells/well), or death (no cells in the well, but used to have cells at earlier time points).

Figure 2. Preferential elimination of the cells with larger nuclei through apoptosis. (A) Representative images of each cell fate. Time-lapse phase-contrast images captured at the indicated time points show that some daughter cells that originated from fused cells undergo apoptosis (black arrow in row 3) whereas others can proliferate like unfused cells (white arrow in row 3). Bar, 20μm. (B) Change of nuclear size following cell fusion. Images of DAPI-stained nuclei were measured by using Axiovision Rel 4.5 software (n=700). Bar indicates median value. (C) Immunoblots of fused and unfused cells were probed with antibodies to PARP-1 and caspase 3. The level of cleaved PARP-1 and activated caspase 3 (black arrows) were increased in fused HeLa cells. Cells were treated with or without z-VAD fmk (10μM) and harvested at 3 day following cell fusion. β-actin: loading control. (D) Preferential death of cells with larger nuclei. The size of nucleus of cells at interphase was measured by the images of cells under microscopic observation (Nikon Ti-E) for 4 days following cell fusion. For data analysis we used NIS elements software. Supplementary figure 2A shows this in more detail. (E) Cell death was partially abrogated by the z-VAD-fmk in fused cells. Cells were seeded in a 12-well plate at a density of $1x10^4$ cells/well and counted by 0.4% trypan blue staining 3 days after cell fusion. Mean ± SD from three independent experiments; *, $p<0.05$ by Student's *t* -test.

Figure 3. Survivin increased in surviving fused cells. (A) Cells were harvested at indicated time points following cell fusion. Protein blots were probed with indicated antibodies. GAPDH: loading control. (B) Immunoblotting was performed with cell lysates derived from fused or unfused stable lines, which were established by using selective medium containing G418(1mg/ml) and Hygromycin(0.8mg/ml) for 3 weeks.

Numbers indicate different stable clones. (C) Cell viability was quantified by using time-lapse images. Cells were transfected with indicated siRNAs at 1 day after fusion and monitored using time-lapse microscope for 60 hours. Cell death events were counted and expressed relative to unfused siControl-transfected cells. n=10 for each group. Mean ± SD from triplicate experiments; *, $p<0.05$ by Student's *t*-test. (D) Effect of survivin on the survival of fused cells. Parental HeLa cells or HeLa cells after electrofusion but without FACS sorting was transiently transfected with siSurvivin (40nM) and siControl (40nM) at 1 day after fusion. After 24h, cells were reseeded and cultured with or without selective medium for 10 days and colonies were counted after crystal violet staining (left lower panel; a representative picture, right panel; graph showing the relative colony number compared to siControl). Cell lysates from the indicated samples at 24h after transfection were subjected to western blot analysis using indicated antibodies (left upper panel). α-tubulin: loading control. Mean ± SD from three independent experiments; ***, $p<0.001$ by Student's *t*-test.

Figure 4. Increased protein stability and cytosolic localization of survivin in fused cells. Fused and unfused cells were cultured by using selective medium containing G418 (1mg/ml) and Hygromycin (0.8mg/ml) for 9 days and harvested at day 9 following cell fusion. (A) The cytoplasmic and nuclear extracts were subjected to western blotting using survivin, lamin B1 and α-tubulin antibodies. Lamin B1 and α-tubulin: fractionation and loading controls. The bar graph shows the quantification of western blot images (Cytoplasmic/Nuclear extracts). Mean ± SD from three independent experiments; **, $p<0.01$ by Student's *t*-test. (B) Immunofluorescence analysis of fused and unfused cells

by using survivin and F-actin antibodies. Bar, 20μm. Quantification of survivin localization was performed using NIS-Elements Imaging Software (Nikon Corporation). Mean ± SD from three independent experiments; **, p<0.01 by Student's *t*-test. (C) Cells were harvested 5 days after cell fusion, and the stability of survivin protein was analyzed by Western blotting of the whole cell lysates prepared from cells after addition of 50μM cycloheximide (CHX). α-tubulin : loading control. Relative levels of survivin were measured by densitometric analysis (right panel).

REFERENCES

1. Duelli DM, Hearn S, Myers MP and Lazebnik Y (2005) A primate virus generates transformed human cells by fusion. J Cell Biol 171, 493-503
2. Ganem NJ, Storchova Z and Pellman D (2007) Tetraploidy, aneuploidy and cancer. Curr Opin Genet Dev 17, 157-162
3. Lu X and Kang Y (2009) Cell fusion as a hidden force in tumor progression. Cancer Res 69, 8536-8539
4. Kerbel RS, Lagarde AE, Dennis JW and Donaghue TP (1983) Spontaneous fusion in vivo between normal host and tumor cells: possible contribution to tumor progression and metastasis studied with a lectin-resistant mutant tumor. Mol Cell Biol 3, 523-538
5. Mortensen K, Lichtenberg J, Thomsen PD and Larsson LI (2004) Spontaneous fusion between cancer cells and endothelial cells. Cell Mol Life Sci 61, 2125-2131
6. Andreassen PR, Lohez OD, Lacroix FB and Margolis RL (2001) Tetraploid state induces p53-dependent arrest of nontransformed mammalian cells in G1. Molecular biology of the cell 12, 1315-1328

7. Vogel C, Kienitz A, Hofmann I, Muller R and Bastians H (2004) Crosstalk of the mitotic spindle assembly checkpoint with p53 to prevent polyploidy. Oncogene 23, 6845-6853
8. Aylon Y and Oren M (2011) p53: guardian of ploidy. Mol Oncol 5, 315-323
9. Vousden KH and Lu X (2002) Live or let die: the cell's response to p53. Nat Rev Cancer 2, 594-604
10. Yu J, Wang Z, Kinzler KW, Vogelstein B and Zhang L (2003) PUMA mediates the apoptotic response to p53 in colorectal cancer cells. Proc Natl Acad Sci U S A 100, 1931-1936
11. Wei MC, Zong WX, Cheng EH et al (2001) Proapoptotic BAX and BAK: a requisite gateway to mitochondrial dysfunction and death. Science 292, 727-730
12. Ho CC, Hau PM, Marxer M and Poon RY (2010) The requirement of p53 for maintaining chromosomal stability during tetraploidization. Oncotarget 1, 583-595
13. Scheffner M, Werness BA, Huibregtse JM, Levine AJ and Howley PM (1990) The E6 oncoprotein encoded by human papillomavirus types 16 and 18 promotes the degradation of p53. Cell 63, 1129-1136
14. Castedo M, Coquelle A, Vitale I et al (2006) Selective resistance of tetraploid cancer cells against DNA damage-induced apoptosis. Ann N Y Acad Sci 1090, 35-49
15. Fukuta K, Kohri K, Fukuda H et al (2008) Induction of multinucleated cells and apoptosis in the PC-3 prostate cancer cell line by low concentrations of polyethylene glycol 1000. Cancer Sci 99, 1055-1062

16. Zhao J, Tenev T, Martins LM, Downward J and Lemoine NR (2000) The ubiquitin-proteasome pathway regulates survivin degradation in a cell cycle-dependent manner. J Cell Sci 113 Pt 23, 4363-4371
17. Li F, Yang J, Ramnath N, Javle MM and Tan D (2005) Nuclear or cytoplasmic expression of survivin: what is the significance? Int J Cancer 114, 509-512
18. Behera B, Mishra D, Roy B et al (2014) Abrus precatorius agglutinin-derived peptides induce ROS-dependent mitochondrial apoptosis through JNK and Akt/P38/P53 pathways in HeLa cells. Chem Biol Interact 222C, 97-105
19. Guo XX, Li Y, Sun C et al (2014) p53-dependent Fas expression is critical for Ginsenoside Rh2 triggered caspase-8 activation in HeLa cells. Protein Cell 5, 224-234
20. Chen X, Duan N, Zhang C and Zhang W (2016) Survivin and Tumorigenesis: Molecular Mechanisms and Therapeutic Strategies. J Cancer 7, 314-323
21. Cheung CH, Huang CC, Tsai FY et al (2013) Survivin - biology and potential as a therapeutic target in oncology. Onco Targets Ther 6, 1453-1462
22. Bai H, Ge S, Lu J, Qian G and Xu R (2013) Hypoxia inducible factor-1alpha-mediated activation of survivin in cervical cancer cells. J Obstet Gynaecol Res 39, 555-563
23. Fortugno P, Beltrami E, Plescia J et al (2003) Regulation of survivin function by Hsp90. Proc Natl Acad Sci U S A 100, 13791-13796
24. Altieri DC (2003) Survivin, versatile modulation of cell division and apoptosis in cancer. Oncogene 22, 8581-8589

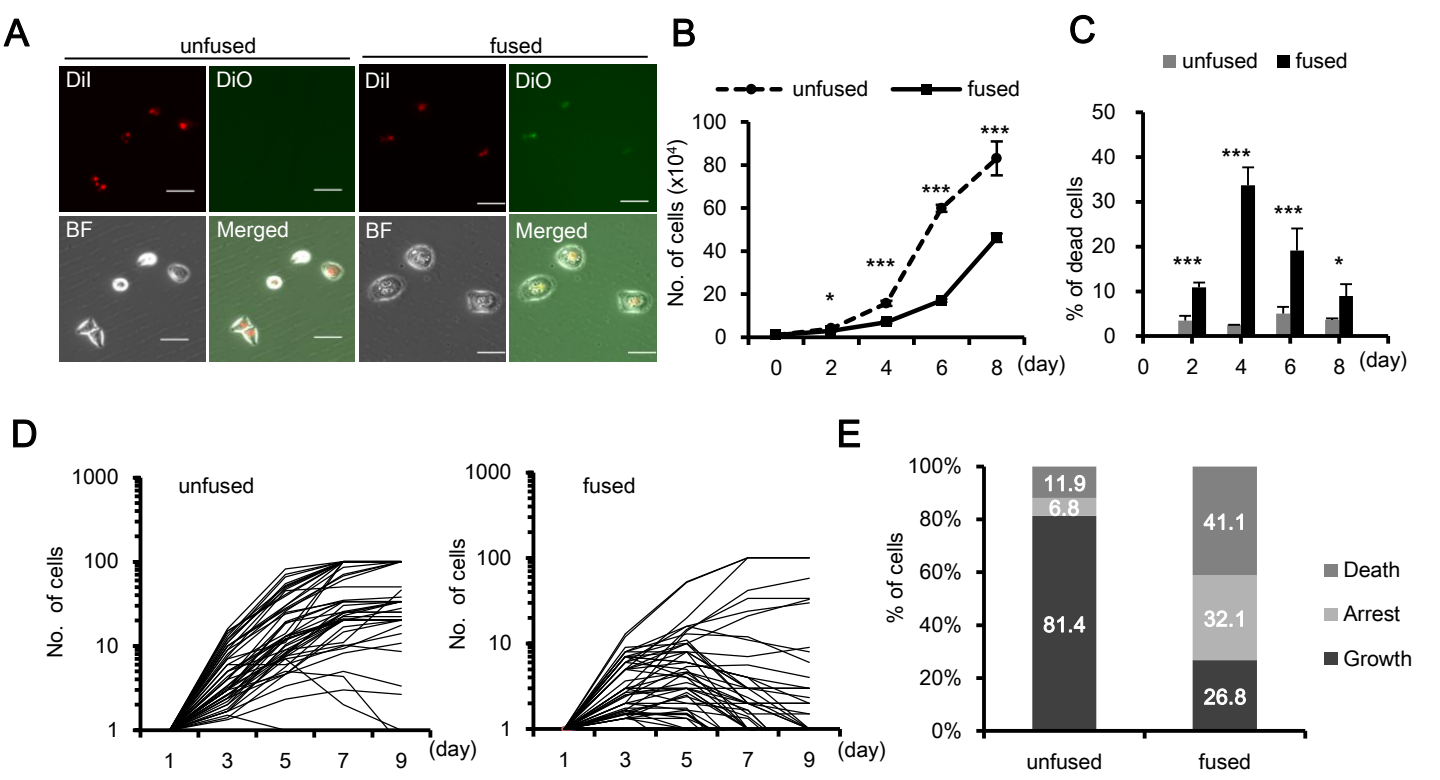
A
unfused
fused
DiI
DiO
BF
Merged
B
unfused
fused
No. of cells (x10⁴)
(day)
C
unfused
fused
% of dead cells
(day)
D
unfused
fused
No. of cells
(day)
E
% of cells
11.9
6.8
81.4
41.1
32.1
26.8
Death
Arrest
Growth
unfused
fused

Figure 1.

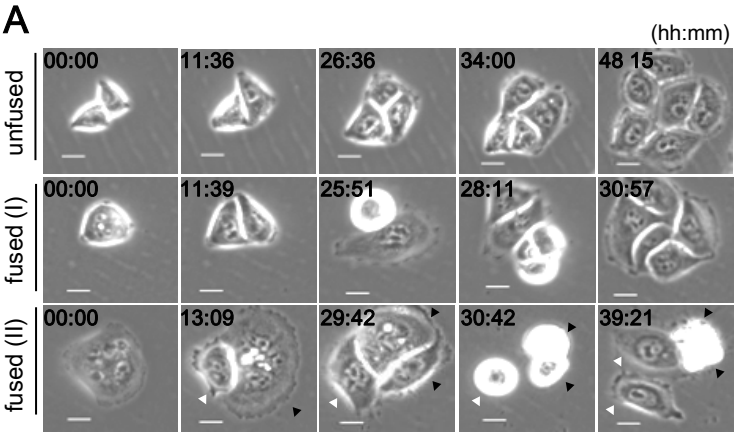
A
(hh:mm)
unfused
fused (I)
fused (II)
00:00
11:36
26:36
34:00
48 15
00:00
11:39
25:51
28:11
30:57
00:00
13:09
29:42
30:42
39:21

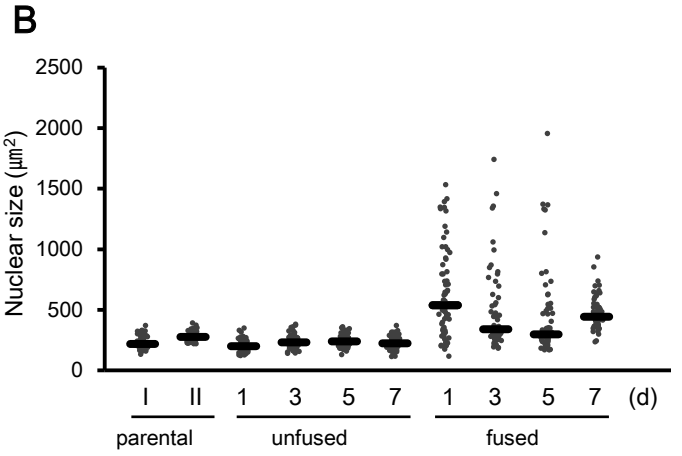
B
Nuclear size (μm²)
2500
2000
1500
1000
500
0
I
II
1
3
5
7
1
3
5
7
(d)
parental
unfused
fused

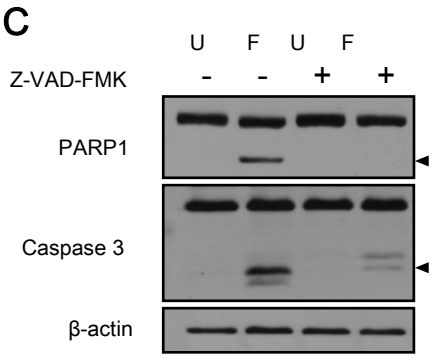
C
U
F
U
F
Z-VAD-FMK
-
-
+
+
PARP1
Caspase 3
β-actin

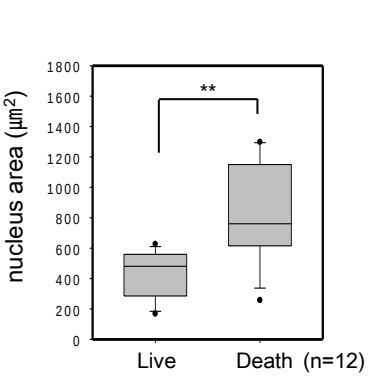
D
nucleus area (μm²)
1800
1600
1400
1200
1000
800
600
400
200
0
**
Live
Death (n=12)

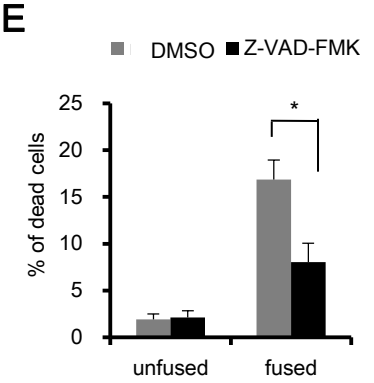
E
DMSO
Z-VAD-FMK
% of dead cells
25
20
15
10
5
0
*
unfused
fused

Figure 2.

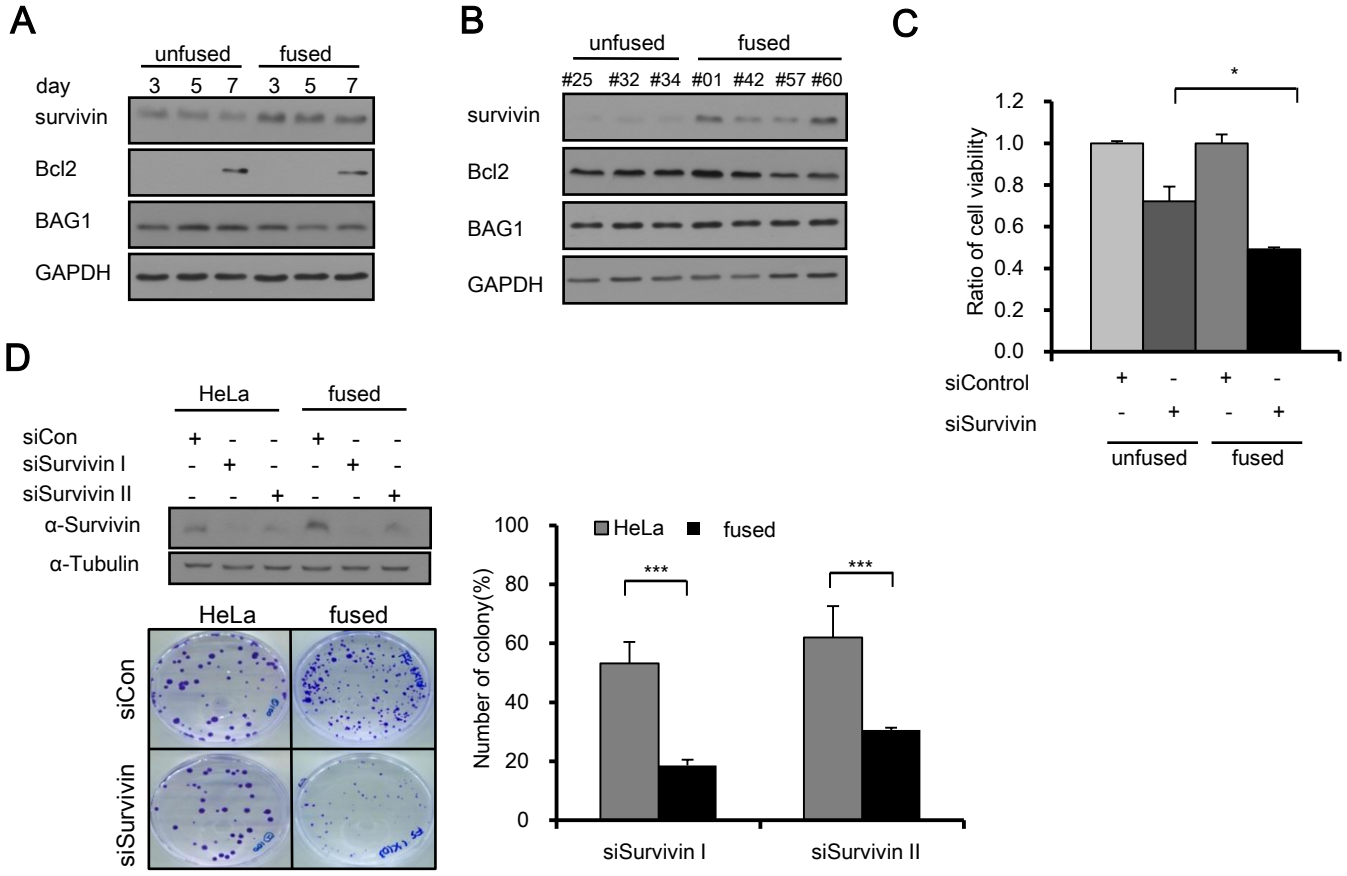
A
unfused
fused
day
3 5 7 3 5 7
survivin
Bcl2
BAG1
GAPDH
B
unfused
fused
#25 #32 #34 #01 #42 #57 #60
survivin
Bcl2
BAG1
GAPDH
C
*
Ratio of cell viability
1.2
1.0
0.8
0.6
0.4
0.2
0.0
siControl
siSurvivin
unfused
fused
D
HeLa
fused
siCon
siSurvivin I
siSurvivin II
α-Survivin
α-Tubulin
HeLa
fused
siCon
siSurvivin
HeLa
fused
Number of colony(%)
100
80
60
40
20
0
***
***
siSurvivin I
siSurvivin II

Figure 3.

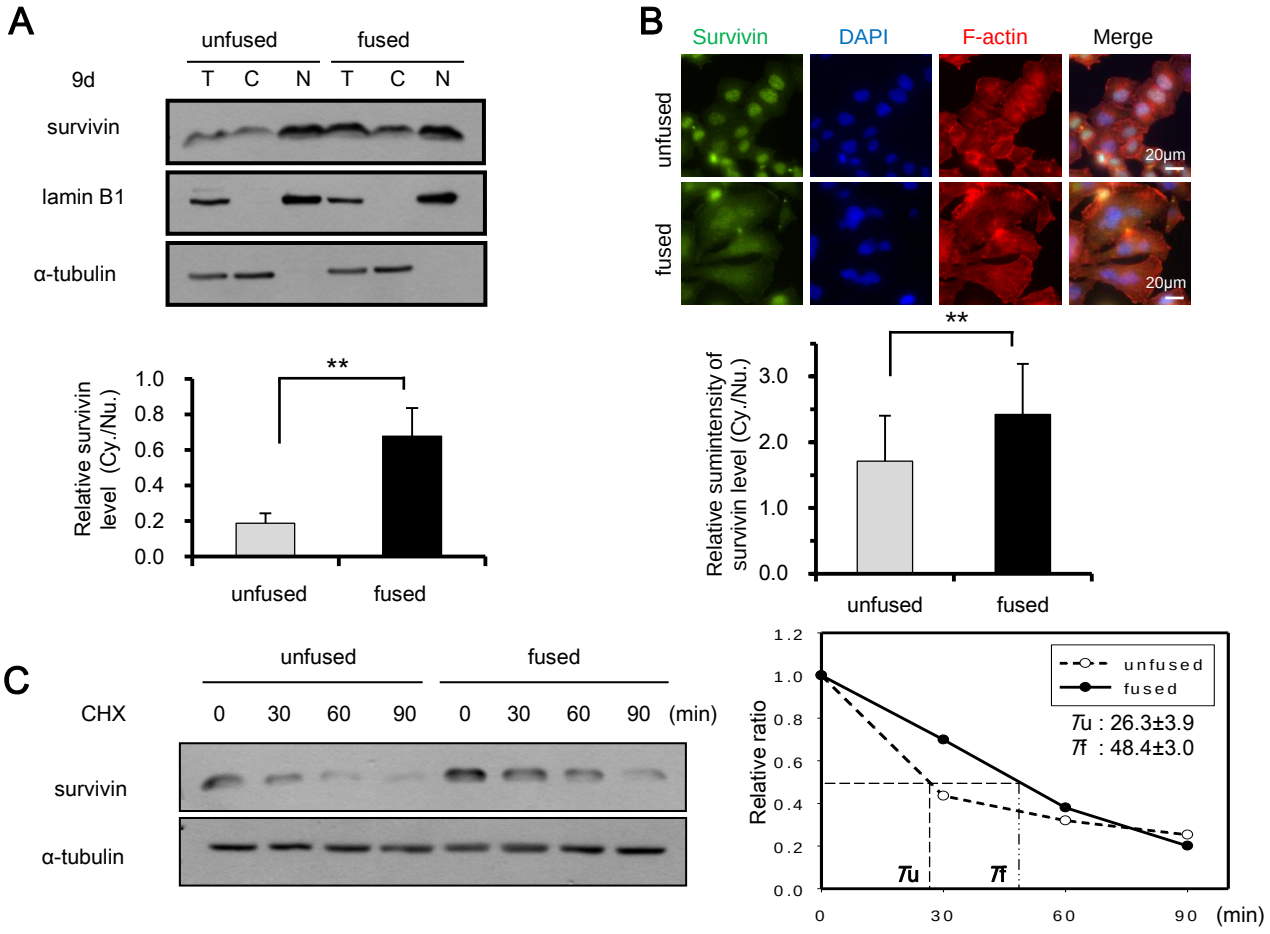
A
unfused
fused
9d
T C N T C N
survivin
lamin B1
α-tubulin
Relative survivin level (Cy./Nu.)
1.0
0.8
0.6
0.4
0.2
0.0
**
unfused
fused
B
Survivin
DAPI
F-actin
Merge
unfused
fused
20μm
20μm
Relative sumintensity of survivin level (Cy./Nu.)
3.0
2.0
1.0
0.0
**
unfused
fused
C
unfused
fused
CHX
0 30 60 90 0 30 60 90 (min)
survivin
α-tubulin
Relative ratio
1.2
1.0
0.8
0.6
0.4
0.2
0.0
unfused
fused
τu : 26.3±3.9
τf : 48.4±3.0
τu
τf
0 30 60 90 (min)

Figure 4.

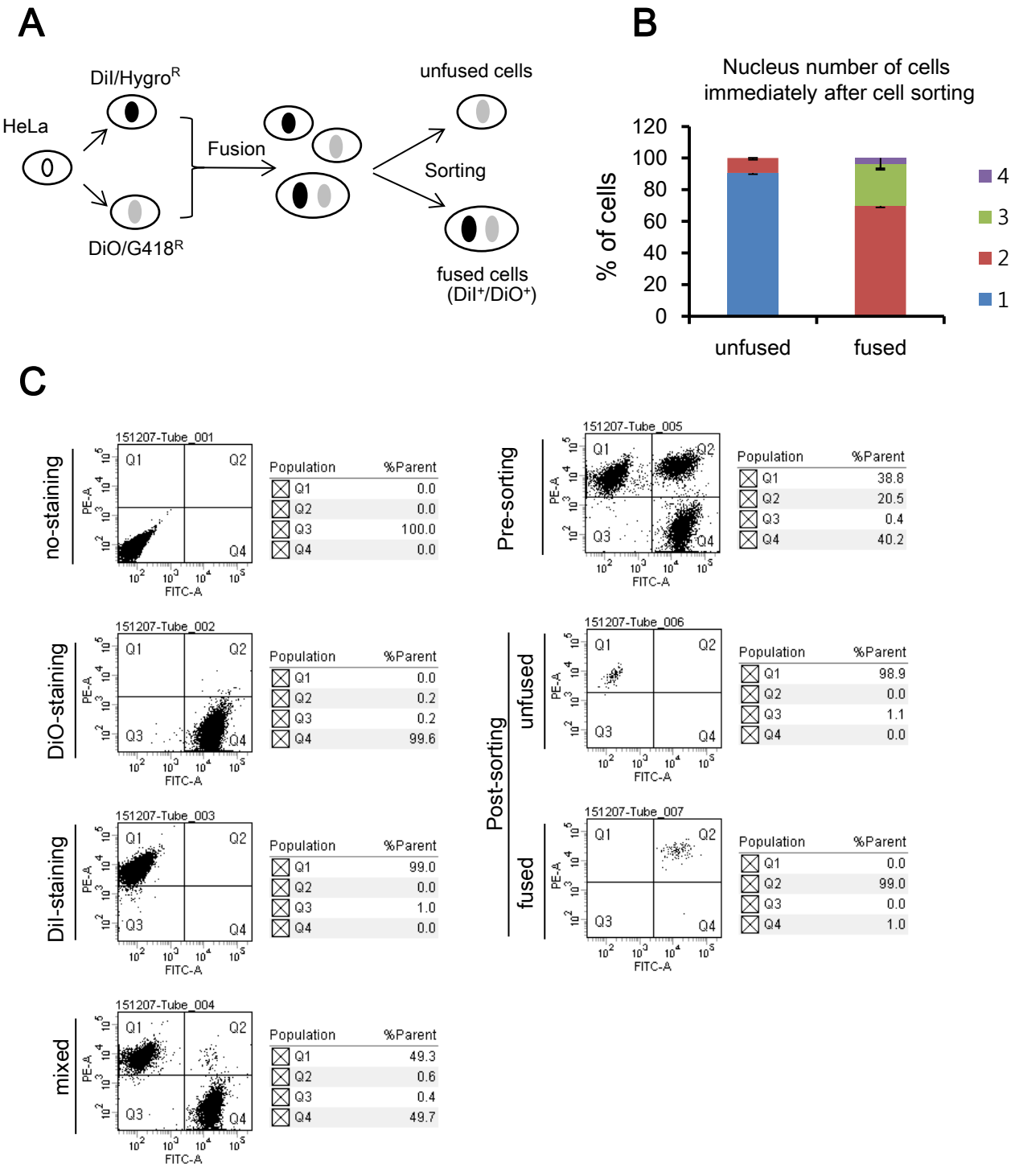

Supplementary Fig.1.

Supplementary Fig.1. Generation and isolation of fused and unfused cells.

(A) Schematic diagram of the cell fusion and selection procedure is shown. Detailed procedure is described in Materials and Methods. (B) Nucleus number of fused and unfused cells was counted with images taken by fluorescent time-lapse microscope (Ti-E Nikon). After cell fusion between H2B-GFP-HeLa and H1-DsRed-HeLa, isolated cells were seeded in a 4-well Lab-Tek chamber slide. Results are given as the mean±SD from three independent experiments. (unfused : n=63, fused : n=23). (C) At 2h after fusion, cells were sorted by FACS and the purity of each isolated population was measured by analytical FACS.

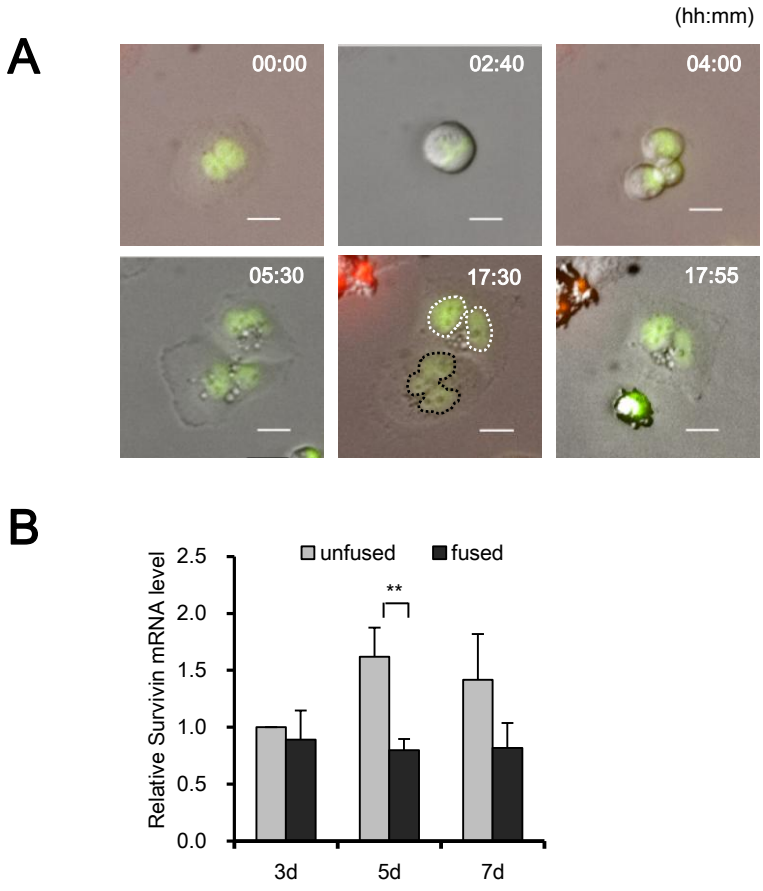

Supplementary Fig. 2. (A) Representative images of meganucleated cell death following cell fusion. The size of nucleus of cells at interphase was measured by the images of cells under microscopic observation (Nikon Ti-E). For data analysis we used NIS elements software. Dotted circles denote a multilobular nucleaus in a single cell. Scale bar: 20μm. (B) Expression of Survivin mRNA for 7 days after cell fusion. Cells were harvested at indicated time points following cell fusion. Relative mRNA level was measured by real-time PCR. Values were expressed as the relative mRNA accumulation corrected using β-actin mRNA as an internal standard. **$p<0.01$ compared to control.

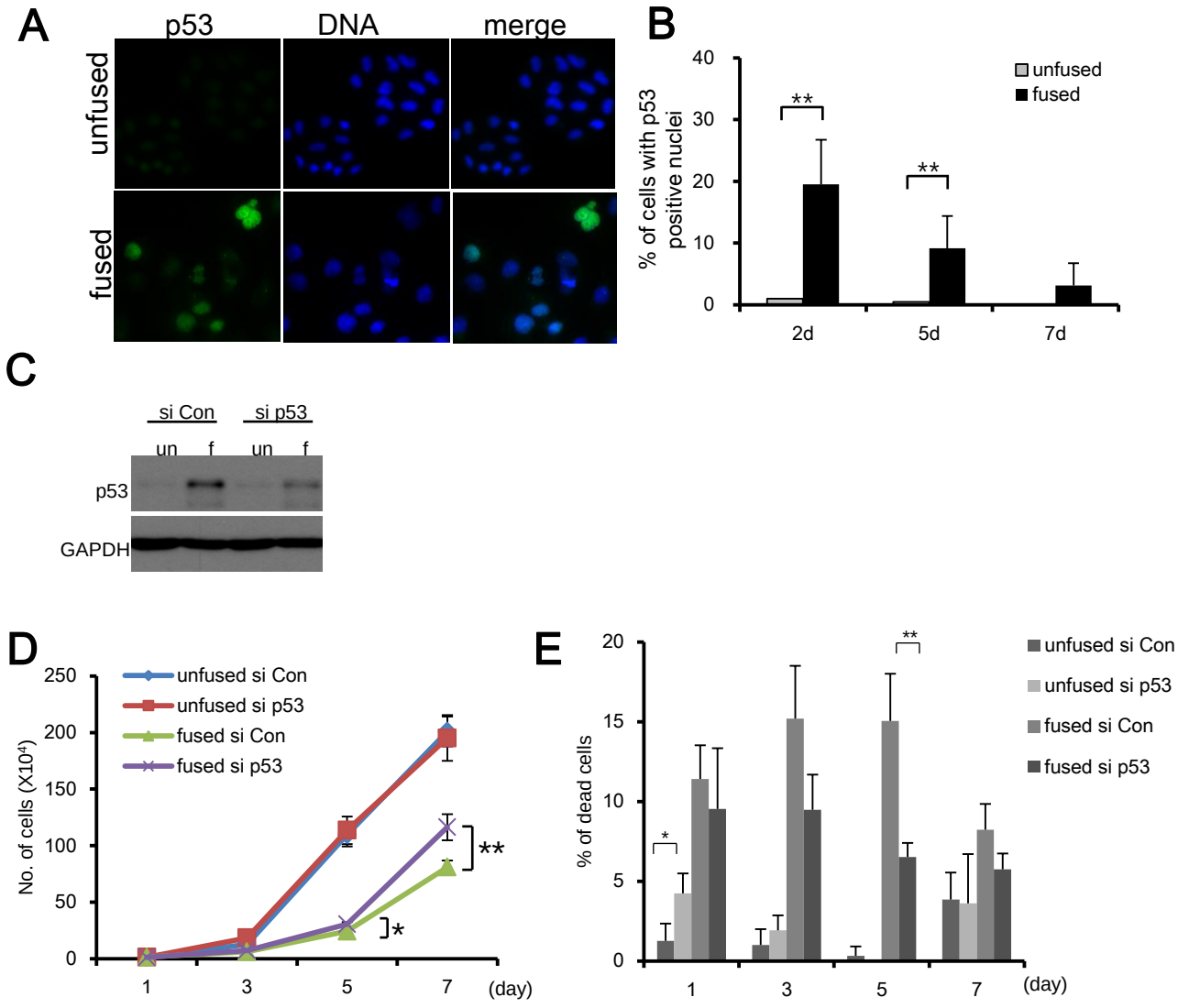

Supplementary Fig. 3. (A) Immunocytochemical staining of p53 in unfused and fused cells at day 2 following cell fusion. (B) The percentage of p53-positive nucleus in unfused and fused cells. Results are given as the mean±SD from three independent experiments (Student's *t*-test, **p<0.01). (C-E) Cells were transfected with indicated siRNAs(100nM) and then subjected to cell fusion process. (C) Cells were harvested at day 5 following cell fusion. Protein blots of fused and unfused cells were probed with indicated antibodies. GAPDH: loading control. Cell number (D) and cell death rate (E) were measured after trypan blue staining. Cells were seeded at a density of $1x10^4$cells per well in 12-well plates and counted at the indicated times. Mean ± SD from three independent experiments; **, p<0.01; *, p<0.05 by Student's *t*-test.

Supplementary information :

Supplementary file 1 : Supplementary information.

Supplementary file 2 : Supplementary figure 1, 2 and 3.

1. MATERIALS AND METHODS

Cell lines, culture conditions and reagents

HeLa cells were cultured in Dulbecco's modified Eagle's medium nutrient mixture F-12 HAM (Sigma Chemical Co.) supplemented with 10% (vol/vol) FBS and 100 U/ml penicillin/streptomycin (Gibco BRL). $G418^R$- or $Hygromycin^R$- HeLa cells were cultured in the presence of 0.3 mg/ml G418 or 0.2 mg/ml Hygromycin B respectively. HeLa cells expressing H2B-GFP and H1-DsRed were cultured in DMEM supplemented with 10% FBS and 100 U/ml penicillin/streptomycin and containing 0.2 mg/ml G418. DiI (D282) and DiO (D275) were purchased from Gibco-Invitrogen (Carlsbad, USA). Cycloheximide (CHX) and z-VAD fmk were purchased from Sigma Chemical Co.

Cell fusion and FACS sorting

HeLa cells were stained with DiI (10 µg/ml) or DiO (10 µg/ml) for 15min at 37°C. Stained or H2B-GFP and H1-DsRed HeLa cells were washed with Ca^{2+}/Mg^{2+}-free phosphate buffered saline (PBS) and resuspended with fresh nonelectrolyte solution (1mM $MgSO_4$, 1mM $CaCl_2$, 0.3M Mannitol) at a density of $2x10^6$ cells per ml. Same numbers of each stained cells were mixed and then used immediately for electrofusion by using ECM 2001 Electro Cell Manipulator (BTX, Harvard Apparatus). Optimized condition of electrofusion was as

follows : AC 20V for 30sec, DC 700V for 70sec, post-fusion AC 20V for 9sec. After then, cells were plated into 10cm culture dish in normal growth media. After 2 hours, cell sorting was performed by using a FACS Aria III Flow cytometer (BD Biosciences).

Limiting dilution analysis of cells

Unfused or fused cells were seeded at a density of 0.5 cell per well in 96 well plate and cultured for 9 days in growth media without selection. The cell number in each well was counted at the indicated times and monitored under microscope.

Small interference RNA

Two independent siRNAs against survivin were used. One was a BIRC5-siRNA (cat.no.1012475) from Bioneer (Daejeon, Republic of Korea) and the other was from Invitrogen with following sequence: 5'-UUUAAGGCUGGGAGCCAGAU GGACGC-3'. p53-specific siRNA was purchased from Bioneer (Daejeon, Republic of Korea) with following sequence : 5'-GACUCCAGUGGUAAUCUAC-3'. Control siRNA was also purchased from Bioneer. Cells were transfected with siRNA using oligofectamine 2000 (Invitrogen).

Antibodies

We purchased following antibodies from Cell Signaling Technology (PARP-1, caspase 3, survivin, Bcl2, BAG1, p53), Santa Cruz (lamin-B1, actin, α-tubulin, GAPDH) or Invitrogen (HRP-conjugated secondary antibodies). Alexa Fluor 488-conjugated secondary antibody

(Molecular Probes) and tetramethylrhodamine (TRITC)-conjugated phalloidin to probe F-actin (SIGMA-ALDTICH) were used for immunocytochemistry.

Live cell imaging

Sorted cells were seeded into 6 cm culture dishes at a concentration of 1.0×10^5 cells per dish. Phase contrast live cell imaging was used with a Zeiss Axiovert 200M fluorescent microscope (Carl Zeiss). Images of unfused (H1–DsRed-HeLa) and fused (H2B–GFP-/H1-DsRed-HeLa) cells were placed in a stage-top incubation chamber and acquired every 3 minutes for 60 hours using by motorized inverted fluorescence time-lapse microscope Nikon Ti-E (Nikon Corporation).

Clonogenic assay

Freshly isolated unfused and fused cells were seeded at different concentrations (from 100 to 2000 for each dish) in 6 cm dish, and cultured for up to 10 days under selection media containing Hygromycin (0.8mg/ml) and G-418 (1mg/ml). Parental HeLa cells were used as control cells, and cultured in normal growth media without selective agents. Colonies were fixed/stained with an aqueous solution containing 0.25% (w/v) crystal violet, 20% (v/v) methanol and counted. Only colonies consist of >30 cells were counted. The effect of survivin knockdown was expressed as the survival fraction (%): survival fraction(%) = 100 x # of colonies in survivin knockdown plate/ # of colonies in control knockdown plate.

Immunocytochemistry

Cells were fixed with 3.7% formaldehyde in PBS and permeabilized with 0.1% Triton X-100 in PBS. Fixed cells were incubated with primary antibody for overnight at 4°C. Cells were

then washed with PBS and incubated with secondary antibody for 1hr at room temperature. For DNA counterstaining, DAPI (Molecular probes) was used.

Quantification of survivin subcellular localization

Quantitative measurement of the signal intensity after immunochemical staining was performed using NIS-Elements Imaging Software (Nikon corporation). The sum intensity (SI) of survivin of total cell (SI_{total}) and that of nuclear area (SI_{nuc}) was measured respectively, and then the cytosolic intensity of survivin (SI_{cyt}) was calculated by the equation ($SI_{cyt} = SI_{total} - SI_{nuc}$).

Real-time PCR

Real-time PCR was carried out in the Bio-Rad CFX 96 Real-Time System (Bio-Rad Laboratories) using KAPA SYBR FAST qPCR Kits (KAPA Biosystems). The mRNA expression level of survivin was normalized using β-actin as an internal control. The 2-ΔΔCT relative quantification method was used to calculate the mean fold expression difference between the groups. The following primers were used: survivin, 5′-CTGCCTGGCAGCCCTTTCTCAA-3′ (forward) and 5′-AATAAACCCTGGAAGTGGTGCA-3′ (reverse); β-actin, 5′-GTGGCATCCATGAAACTACAT-3′(forward) 5′-AACGCAGCTCAGTAACAGTC-3′ (reverse).

2. SUPPLEMENTARY DATA LEGENDS

Supplementary Fig. 1. Generation and isolation of fused and unfused cells. (A) Schematic diagram of the cell fusion and selection procedure is shown. Detailed procedure is described in Materials and Methods. (B) Nucleus number of fused and unfused cells was counted with images taken by fluorescent time-lapse microscope (Nikon Ti-E). After cell fusion between H2B-GFP-HeLa and H1-DsRed-HeLa, isolated cells were seeded in a 4-well Lab-Tek chamber slide. Results are given as the mean±SD from three independent experiments. (unfused : n=63, fused : n=23). (C) At 2h after fusion, cells were sorted by FACS and the purity of each isolated population was measured by analytical FACS.

Supplementary Fig. 2. (A) Representative images of meganucleated cell death following cell fusion. The size of nucleus of cells at interphase was measured by the images of cells under microscopic observation (Nikon Ti-E). For data analysis we used NIS elements software. Dotted circles denote a multilobular nucleaus in a single cell. Bar, 20μm. (B) Expression of Survivin mRNA for 7 days after cell fusion. Cells were harvested at indicated time points following cell fusion. Relative mRNA level was measured by real-time PCR. Values were expressed as the relative mRNA accumulation corrected using β-actin mRNA as an internal standard. **$p < 0.01$ compared to control.

Supplementary Fig. 3. (A) Immunocytochemical staining of p53 in unfused and fused cells at day 2 following cell fusion. (B) The percentage of p53-positive nucleus in unfused and fused cells. Results are given as the mean ± SD from three independent experiments (Student's *t*-test, **$p < 0.01$). (C-E) Cells were transfected with indicated siRNAs (100nM) and then subjected to cell fusion process. (C) Cells were harvested at day 5 following cell fusion. Protein blots of fused and unfused cells were probed with indicated antibodies.

GAPDH: loading control. Cell number (D) and cell death rate (E) were measured after trypan blue staining. Cells were seeded at a density of $1x10^4$cells per well in 12-well plates and counted at the indicated times. Mean ± SD from three independent experiments; **, $p < 0.01$; *, $p < 0.05$ by Student's *t*-test.